Aalto University

Franco, Ana; Neves, Carlos Marques; Quintao, Carla; Vigario, Ricardo; Vieira, Pedro

Singular Spectrum Analysis of pupillometry data. Identification of the sympathetic and parasympathetic activity

Conference on Electronics, Telecommunications and Computers – CETC 2013

Singular Spectrum Analysis of pupillometry data. Identification of the sympathetic and parasympathetic activity

Ana Franco[a,b], Carlos Marques Neves[c], Carla Quintão[a,d], Ricardo Vigário[e], Pedro Vieira[a,b] *

[a]Department of Physics, Faculty of Sciences and Thecnology, NOVA University of Lisbon, Quinta da Torre, 2829-516 Caparica, Portugal
[b]Atomic Physics Center, Faculty of Sciences and Thecnology, NOVA University of Lisbon, Portugal
[c]Faculty of Medicine, University of Lisbon, Portugal
[d]Institute of Biophysics and Biomedical Engineering, Faculty of Sciences, University of Lisbon, Portugal
[e]Department of Information and Computer Science, Aalto University School of Science, Finland

Abstract

The pupil shows a fast dynamical adaptation to external light changes, in order to potentiate visual perception. It contracts in high luminosity environments, so as to limit the quantity of photons that reach the retina (miosis) and dilates in environments with little luminosity, thus increasing the number of photons in the retina (mydriasis). Hence, the pupil acts as a normalizer of the quantity of light that enters the optical system. These pupillary movements are controlled by the action of smooth muscles, which are associated with the sympathetic (SNS) and parasympathetic autonomous nervous systems (PsNS). Therefore, the study of the pupillary dynamics can lead to inferences on the functioning of those two antagonist systems and their involvement in pupillary control. In addition, our study may prove clinically helpful in determining a patient's level of consciousness, as well as identifying certain diseases, such as sleep disorders, photophobia, schizophrenia, Adie syndrome, Alzheimer's and Parkinson's disease. With a clear goal in its clinical applications, we focus our research in the identification of the frequency intervals pertaining to the action of the autonomous nervous system, as well as their individual sympathetic and parasympathetic roles.
We analyze high-resolution, non-invasive pupillometric signals, both in a basal condition and as a response to visual flashes or to the application of a cold stimulus. We use Singular Spectrum Analysis (SSA) to identify the frequencies of interest related to the actions of the SNS and PsNS. In addition, and as a complementary means of frequency analysis, we also use the more classical wavelets analysis. We find out that SSA is an ideal tool for the identification of the desired frequencies in stake. The agreement between the outcomes of both analyses supports our conclusions regarding the autonomous nervous system.

* Corresponding author. Tel.: +351 212948576; fax: +351 212948549.
E-mail address: pmv@fct.unl.pt

Nomenclature

SSA   Singular Spectrum Analysis
PSD   Power Spectral Density
LF/HF Low and High Frequency
ECG   Electrocardiogram
PCD   Pupil Contour Detection
SNS   Sympathetic Nervous System
PsNS   Parasympathetic Nervous System
PCA   Principal Component Analysis

1. Introduction

The autonomic nervous system has the function of regulating a large portion of the visceral functions of the body, in response to external changes, through its association with smooth muscles, cardiac muscle and glands. In this respect, one of the functions of the autonomic nervous system is also to control the dynamics of the pupil[1].

The main function of the pupil is to control the amount of light incident on the retina[2],[3]. It has the ability to adapt to changing external luminosity conditions: it contracts in high luminosity environments, and dilates in environments with little luminosity[4]. The pupillary contraction occurs through the action of parasympathetic nerves, resulting in the contraction of circular fibers of the iris sphincter. Similarly, pupillary dilation occurs through stimulation of peripheral sympathetic nerves, which results in the contraction of the radial fibers of the dilator muscle of the iris[4]. Therefore, the eye is innervated by nerve fibers from the autonomic nervous system, whose activation and deactivation allows for an efficient control of the pupil diameter. Thus, the study of the dynamics of the pupil allows for the inference of operating characteristics of the sympathetic and parasympathetic nervous systems (SNS and PsNS, respectively).

Several studies in heart rate variability[5],[6] quantify the balance between the SNS and the PsNS' action, through a relation between their respective power spectral densities (PSD). A major limitation in those studies is the implicit assumption of direct proportionality between those two terms. It has been shown that the true dynamics of the autonomic nervous system follows instead a rather non-linear behavior, c.f.[5]. Therefore, the aforementioned studies characterized the relationship between the SNS and the PsNS, through the ratio between low frequencies (LF) and high frequencies (HF). They established that the range LF (0.04-0.15Hz) is associated to a mixture of sympathetic and parasympathetic activity, whereas the range HF (0.15-0.4Hz) is mostly associated to the parasympathetic activity[5],[7]. To mitigate the limitations of the original PSD method, a weighted ratio has been proposed instead[6]:

$$\frac{LF}{HF} = \frac{0.5 \times \text{parasympathetic activity} + 0.25 \times \text{sympathetic activity}}{0.9 \times \text{parasympathetic activity} + 0.1 \times \text{sympathetic activity}}. \tag{1}$$

Various stimuli types are often used, when studying pupil dynamics. Since they affect differently the autonomic nervous system, a concomitant variability in pupillary response is often observed. As an example, in response to flash stimuli, there is an increased parasympathetic nervous activity, followed by the activation of the SNS[4]. At pupillary level, this corresponds to a contraction, followed by a dilation[4],[8]. If one uses a cold stimulus, *e.g.*, by immersing the subject's hand in icy water, studies indicate an increase in muscle sympathetic nerve activity[9],[10]. In this way, it is therefore possible to isolate behaviors originating from SNS and PsNS.

Pupillary reactivity is measured by pupilometers, which have been used, for example, to evaluate the cholinergic deficiency in Alzheimer's and Parkinson's diseases[11],[12]. Through measures of pupil size and mobility, pupillometry was shown to be a rather sensitive tool to investigate cholinergic deficits, associated with cognitive disorders.

In this study we used a computerized pupilometer, developed in house[13], capable of high spatial and temporal resolutions. We have also developed measuring and analysis methods for such data. As suggested in[4], our setup records and analyzes various features from the pupil, using CCD cameras (charge-coupled device) as detectors.

Here, our main proposal is the use of singular spectrum analysis (SSA) for the identification of frequencies of interest from pupillometric data. This technique is rooted on the principal component analysis (PCA) of embedded copies of the signals, and is capable of revealing intrinsic dynamical factors in the data[14]. It can be used to model and analyze nonlinear time series[15]. Inherited from its PCA derivation, the components found are uncorrelated; from the embedded nature of the analysis comes the dynamical structures in the components.

Unlike Fourier analysis, which assumes sinusoidal bases, or Wavelet analysis, for which we need to determine a priori a suitable set of bases, SSA estimates these directly from the data's dynamics. This renders SSA a good candidate for data exploration, when little information exists on the sought dynamics. The outcome of SSA can as well be used to optimize the choice of wavelet bases. Another advantage of SSA is that only two parameters need to be determined beforehand: in the decomposition stage, the window length; in the reconstruction, the grouping strategy for the estimated components[14].

2. Materials and methods

2.1. Data set

In this study, we used two different groups of volunteers, labeled G1 and G2. In the first, with 15 subjects (6 females, and a mean age of 25 ± 2 years), underwent flash visual stimulation, whereas G2, with 12 subjects (7 females, and a mean age of 28 ± 11 years) was used to assess basal conditions and responses to cold stimuli (icy water). Both groups were composed of healthy subjects, without any eye disease or the influence of any drugs that compromise pupillary action. Some exclusion criteria were established for group G2. Acquisitions of individuals with blue eyes and very long eyelashes were excluded, because pupillary contours were harder to detect. Subjects that blink too often were also excluded since that action changes significantly the shape of the pupil. Our model of pupil dynamics assumed a fixed shape throughout the experiment, since only aperture was to be analyzed.

2.2. Instrumentation

We used the computerized pupilometer developed by Gonçalo Leal[13], which is illustrated in Figure 1. It is a non-invasive monocular pupilometer, with high acquisition rate, 30 Hz, and capable of measuring the variation of pupillary area in high and low luminosity environments. This device consists of an infrared CCD camera (JAI CM-140GE), comprising a high-resolution solid state sensor. A manually adjustable zoom lens allows for a suitable fitting of the equipment to the subject's eye. The complete setup comprises also an infrared light to illuminate the anterior segment of the eye. Two polarizing filters, one ring-shaped, placed in front of the infrared light, and another circular shaped, placed in front of the lens, prevent reflection effects on the eye. Associated with this measurement system, a stroboscopic light was used for the required flash stimulation. A mechanical support adjusts the subject's head position in relation to the measurement device[13].
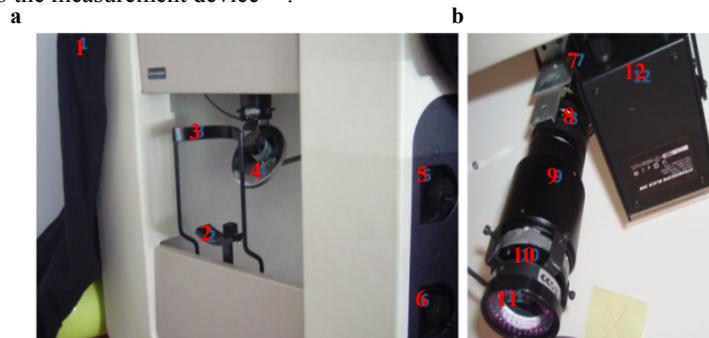

Figure 1 – (a) Mechanical infrastructure of pupilometer: 1 – opaque cloth; 2 - mechanical support of chin; 3 - mechanical support for forehead; 4 – mirror; 5 - lateral screw for horizontal adjustment; 6 - lateral screw for vertical adjustment. (b) Optic system of the pupilometer: 7 - chamber; 8 - zoom lens; 9 - lens polarizer; 10 - illuminator polarizer; 11 - illuminator; 12 - stroboscope.

2.3. Experimental setup

Four protocols were used: one, with no external stimulation, produced basal information; another included the immersion of the subject's hand in icy water; in another, visual flashes were used; and in the final protocol, ECG recordings were acquired, together with the pupillometric information. In this last protocol, cold stimulus was employed. All protocols included a pre-acquisition phase, to control the relative position of the subject to the

pupilometer. During pupillometry acquisition, subjects were instructed to avoid moving their heads or making intermittent eye movements. Also, it was important to keep the eye as open as possible, during the maximum period of time. After image acquisition, pupillary delineation was performed through PCD software[16], and pupillary variations recorded. In addition, median filtering and curve fitting were applied to the pupil contours, to remove outliers in the data.

2.4. Singular Spectrum Analysis

Singular Spectrum Analysis is a signal processing technique capable of capturing the intrinsic oscillation modes of a signal. It is based on a PCA projection of embedded data, and decomposes a given signal on three types of components: trends, periodic components and noise. The trend components give information about slow variations of the signal amplitude throughout time. Each periodic component is related to a given oscillation mode within the signal. The noise is assumed to be associated with the lesser energetic components[15].

SSA has four main steps: embedding, decomposition, grouping and reconstruction. During the embedding stage, L delayed copies are constructed from the N elements of the signal $[x_1, x_2,\ldots, x_N]$, to construct a L x M matrix, defined as: $X_{\text{lag}}=[x_1, x_2,\ldots, x_M; x_2, x_3,\ldots, x_{M+1};\ldots; x_L, x_{L+1},\ldots, x_N]$, where the window length L is a parameter, defined by the user, and $M = N - L + 1$. In the decomposition step, principal directions are found through diagonalization of the covariance matrix of X_{lag}. This decomposition results in a set of eigentriples (j_i, U_i, V_i). j_i is the square root of the ith eigenvalue of the covariance matrix, and U_i its corresponding eigenvector. V_i is defined through: $j_iV_i = X_{\text{lag}}X_{\text{lag}}^{\text{T}}U_i$ [15],[18]. In the grouping step, the eigentriples are combined, in order to establish the desired trend, periodic components and noise. Such grouping requires the use of a similarity measure, to be applied to the all eigentriples. A common such measure, used also in this study, is the weighted correlation (w-correlation) matrix[15]. The first group often displays trend information, and is followed by a set of oscillatory components. The last entries in the w-correlation matrix usually correspond to noise. In the final step, reconstructed time series are produced by backprojecting each one of the grouped eigentriples.

In this work, we performed SSA decomposition of temporal evolutions of pupillary areas with the CaterpillarSSA 3.40 software[17]. The goal, as stated earlier, was to isolate the activities of the SNS and the PsNS from the original signal, through varying experimental conditions.

Figures 2 (a) and (b) show pupillometry variations with cold and flash stimuli, respectively. It is known that cold stimulation activates the SNS, whereas flash stimulation results in an increase in parasympathetic nervous activity, followed by sympathetic activation. So, to identify components related to the action of SNS, we analyzed the dilatations resulting from the application of ice stimuli (represented in green on Figure 2 (a)) and flash stimuli (represented in blue on Figure 2 (b)). To identify components related to the action of the PsNS, we analyzed the contractions resulting from the application of flash stimuli (illustrated in orange on Figure 2 (b)). To study the contribution of the SNS and the PsNS, in basal conditions, we analyzed also pupillometric data without external stimulation (Figure 2 (c)).

In line with the suggested in the literature[15],[18], the window length, L, was chosen as an integer fulfilling the conditions: $1 < L < N$ and $L \leq N/2$. Since we are looking for very low frequencies, less than 1Hz, we used the largest allowed window length. Taking the signal represented in Figure 2 (a) as an example, with a length of 929 samples, we considered a window length of 464 (929/2). Therefore, we found 464 components, each of which characterized by its eigentriple. The w-correlation matrix of the first twenty eigentriples is shown in Figure 3. The remaining ones were considered noise. At least 90% of the total variance in the data was explained by the retained components.

In Figure 3, white corresponds to a correlation of 0, and black to 1. The block structure in the figure clearly highlights the uncorrelated structure of the various groups. Therefore, one can conclude that the first eigentriple clearly separates one component, resulting corresponding to the trend. The eigentriples (2,3), (4,5), (6-9), (10,11), (12,13), (14,15), (16,17) and (18,19) for other discriminated groups. The first six reconstructed components are presented in Figure 4. The frequency content of each reconstructed component is displayed in Table 1.
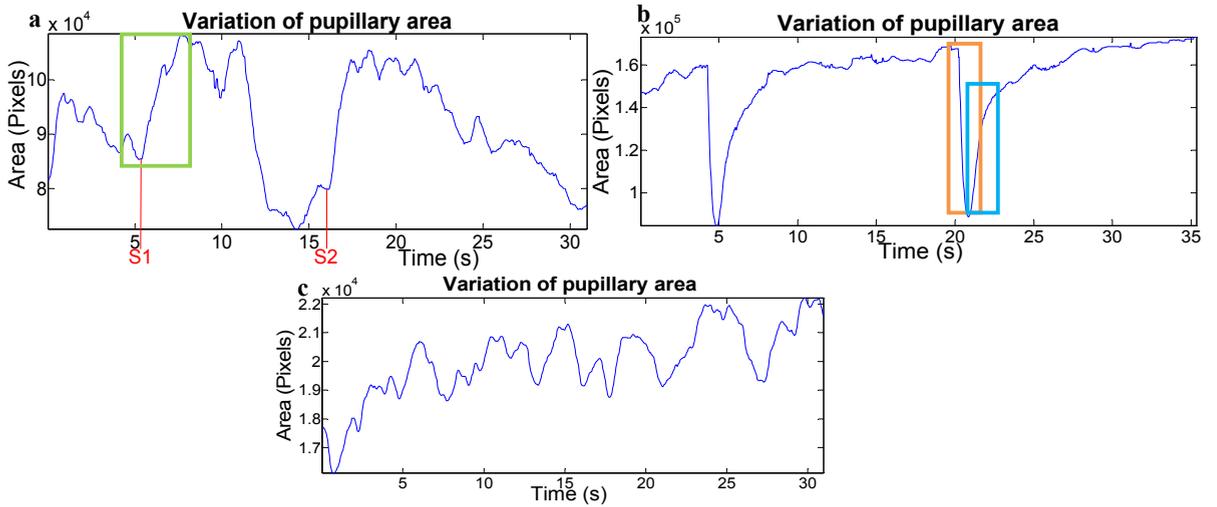
Figure 2 – Analyzed pupillometry signals. (a) Integral signal of the variation of pupillary area with cold stimuli. The instants represented by S1 and S2 correspond to consecutive stimuli applications. The dilation caused by the first stimulus is represented in green. (b) Integral signal of the variation of pupillary area with flash stimuli. The pupillary contraction caused by the first stimulus is represented in orange; and the pupillary dilatation caused by the second stimulus is represented in blue. (c) Variation of pupillary area on basal conditions.
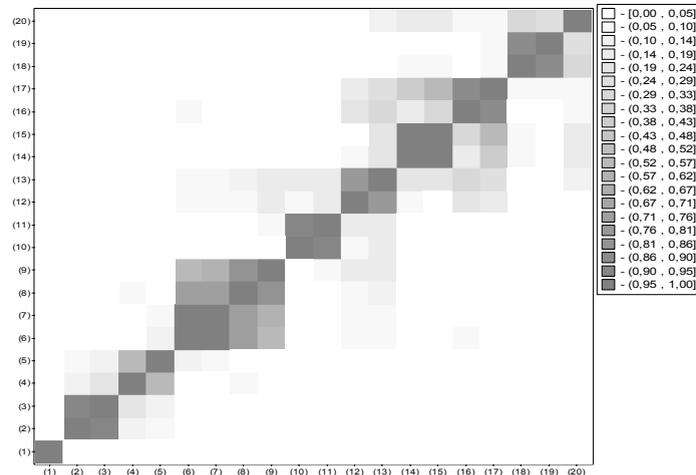

Figure 3 – W-correlation matrix of the first twenty eigentriples found from pupillometric data collected with cold stimulation.
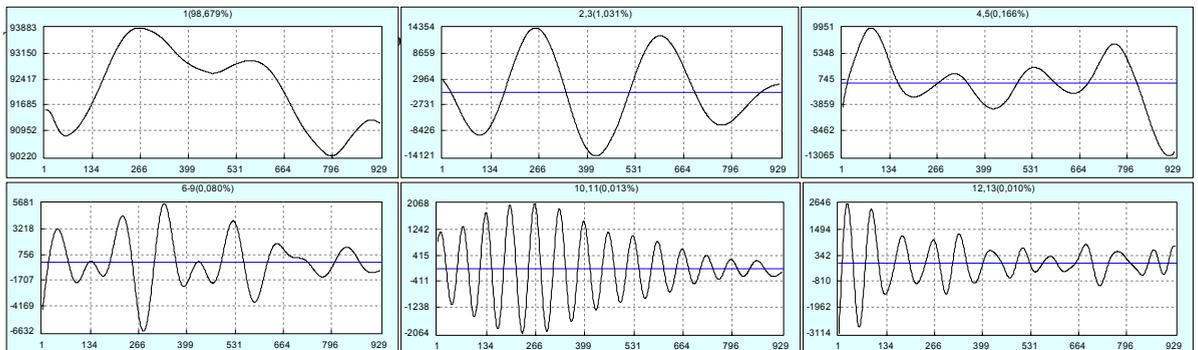

Figure 4– Representation of first 6 reconstructed periodic components.

Reconstructed Components	2	3	4	6	5
Eigentriples	2-3	4-5	6-9	12-13	10-11
Number of cycles	3	4	8.2	11.5	13.6
Frequency (Hz)	0.01	0.13	0.27	0.37	0.44

2.5. Wavelets Analysis

The pupillometric signals were also analyzed with wavelets, using the MATLAB signal processing toolbox. Wavelet analysis was used as a complementary method to SSA, and produced a time-frequency decomposition of each signal, based on their frequency contents. This decomposition gave information about which predominant frequencies were present at a given time. In our study, and due to its temporally smooth and symmetric characteristics, we chose the Daubechies wavelet family of order 10. To produce an efficient denoising of the data, we reconstructed our signals using an 8 level approximation. Finally, a color plot, which allowed to localizing temporally the characteristic frequencies of each reconstructed component was drawn.

3. Results and discussion

3.1. Singular Spectrum Analysis

Through SSA, we identified characteristic frequencies for SNS and PsNS, from both types of stimuli, *i.e.,* cold and flash. These, together with dilation and contraction times, are displayed in Table 2. Dilation and contractions are measured via the rise and fall of the pupillary area, respectively.

Table 2 - Summarizing table of the duration and frequency in pupillary area variations, as a function of the applied stimulus.

Type of stimuli	Stimulus effect	Average ± standard deviation of the frequencies (Hz)	Average ± standard deviation of the times (s)
Cold	Rising	0,46 ± 0,09	1,35 ± 0,35
Flash	Rising	0,47 ± 0,10	1,29 ± 0,31
	Descent	0,73 ± 0,09	0,60 ± 0,14

From the table above, it is clear to see that both the rising times and rising frequencies are independent from the type of stimulus applied. So, one could assume that, in both situations the pupillary dilation is controlled by the activation of the SNS alone.

As for the signal's descent, corresponding to pupillary contraction due to the application of the flash stimulus, we argue that it is mainly related to an increasing in PsNS activity.

Since the ratio LF/HF (equation 1) is known from other physiological studies, namely from heart rate variability[5],[7], it is possible to compare the frequencies found in this study, for the sympathetic and parasympathetic activities, with those found in such earlier studies. A typical value for the LF/HF ratio, calculated from literature dealing with cardiac data, is 0.62±0.02. If we compute a similar measure using our pupillary signals with flash stimuli, we obtain the value 0.67±0.03. Both intervals intersect, suggesting an agreement between both ways to assess the sympathetic and parasympathetic activities.

Interestingly, and although it is not designed for that purpose, pupillometric information could also estimate other frequencies of interest. In fact, in the basal experimental setup, we found that respiration had a frequency in the range 0.2-0.3 Hz[19], and the heart rate between 1 and 1.5 Hz[20]. The latter results were validated via simultaneous electrocardiographic recordings. There was a clear agreement between the electrophysiological measurements (1.47±0.22 Hz) and the SSA processed pupillometric signals (1.40±0.19 Hz).

3.2. Wavelets Analysis

The wavelets analysis corroborates what was found through SSA analysis. We observed that the fifth and sixth approximation levels of the wavelet decomposition had frequency contents in line with the ones reported in SSA, and associated with SNS and PsNS activities. The analysis is illustrated in Figure 5, where all 8 level approximations are depicted (upper frame), together with their temporal strengths (lower frame).
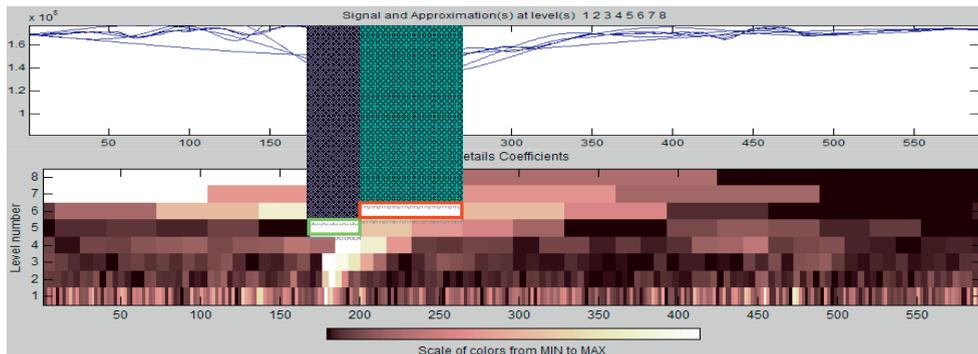

Figure 5 - The top graph corresponds to the signal and the approximation of the eight levels of reconstruction. The lower graph depicts the temporal activation strength of each detail level. Two periods of levels of interest, d5 and d6, are highlighted in green and red, respectively.

As shown in the Figure 5, component d_5 has increased amplitude (white) during pupillary contraction. The frequency of this component is 0.61 Hz, which is in line with the frequency determined for the PsNS activity through SSA. Such agreement increases our belief this is the component responsible for the pupillary contraction, and could therefore be related to the parasympathetic activity.

On the other hand, component d_6 shows higher amplitude during pupillary dilation. The frequency of this component is 0.31 Hz, which is comparable with the frequency determined for SNS by SSA. As before, this information strengthens our belief that such frequency is associated to pupillary dilatation, and thus, to sympathetic activity.

4. Conclusions

A good evaluation of the autonomic nervous system activity is essential for the diagnosis of several neurodegenerative diseases. Our study showed that such information can also be harvested through pupillometry analysis. In particular, frequencies found for sympathetic ($0,47 \pm 0,01$ Hz), as well as parasympathetic activity ($0,73 \pm 0,09$ Hz) are in line with the expected values in literature.

By calculating the ratio between low and high frequency components in the data, we were also able to shed some light into the balance between the activities in the SNS and PsNS. In particular, we showed that pupillary LF/HF ratio estimation is rather close to that found for cardiac data, as reported in the literature. Such finding clearly validates our pupillometric estimating strategy as a viable alternative to study the autonomic nervous system.

Methodologically, we have shown that SSA is a very efficient tool for the identification of the intrinsic oscillation modes in pupillary dilation and contraction, as a response to external stimulation. SSA has clearly an increased algorithmic complexity, when compared to more standard approaches such as wavelet analysis, since it comprises, in addition to a projection step, the estimation of its projectors/bases, which are given for the wavelets. Yet we note that, for the dimensions of the analyzed data, both processes are rather instantaneous, suggesting that the increase in complexity does not affect significantly the choice of methodologies to use. Furthermore, SSA and wavelet analysis give agreeing frequency estimation results, in spite of their different strengths and theoretical backgrounds. This suggests that a combined use of such techniques may lead to a robust assessing tool for the analysis of the action of the autonomous nervous system, as measured through pupillometric recordings.

Finally, this study opens also new vistas for the diagnosis of diseases hindering the normal functioning of the autonomic nervous system. One may evaluate any deviation from normal values, both in the estimated frequencies for the SNS and PsNS's activities, and in the balance between both systems. To establish this possible clinical use,

further studies will be needed, including subjects suffering from various neurodegenerative pathologies. Patterns of normal and pathological behavior can then be proposed. With these patterns established, our analysis could be included in ophthalmic instrumentation, allowing for an immediate evaluation of the functioning of the autonomic nervous system, during regular screening sessions.

Since the autonomic nervous activity alters with the state of consciousness of a subject, an interesting corollary of this study would be a smartphone-like application that could integrate the equipment of first-aid teams. This tool would allow, for example, for a rapid assessment of the state of consciousness of victims of an accident.

Ocular movement proved to be one of the main sources of pupillometric evaluation errors. To avoid them, we propose the use of eyes drops, in order to get ocular relaxation and lubrication, hence mitigating the need for movement.

Acknowledgements

References

[1] A. C. Guyton and J. E. Hall, Tratado de Fisiologia Médica, 10a ed. Rio de Janeiro: Guanabara Koogan, 2002, pp. 558–559.
[2] D. D. Chiras, Human Biology, 6th ed. Sudbury: Jones and Bartlett Publishers, 2008.
[3] A. Alm and P. L. Kaufman, "The Pupil," in Adler's - Physiology of the eye - Clinical Application, 10th ed., Mosby: Elsevier, 2002, pp. 713–743.
[4] R. Bannister and C. J. Mathias, "Pupil function: test and disorders," in Autonomic Failure : A Textbook of Clinical Disorders of the Autonomic Nervous System, 4th ed., Oxford: University Press, 1999, pp. 245–253.
[5] Y. Zhong, K.-M. Jan, K. H. Ju, and K. H. Chon, "Quantifying cardiac sympathetic and parasympathetic nervous activities using principal dynamic modes analysis of heart rate variability", American journal of physiology. Heart and circulatory physiology, vol. 291, no. 3, pp. H1475–83, Sep. 2006.
[6] G. E. Billman, "The LF/HF ratio does not accurately measure cardiac sympatho-vagal balance", Frontiers in physiology, vol. 4, no. February, p. 26, Jan. 2013.
[7] Y. Zhong, H. Wang, K. H. Ju, K.-M. Jan, and K. H. Chon, "Nonlinear analysis of the separate contributions of autonomic nervous systems to heart rate variability using principal dynamic modes", IEEE transactions on bio-medical engineering, vol. 51, no. 2, pp. 255–62, Feb. 2004.
[8] Hachol, W. Szczepanowska-Nowak, H. Kasprzak, I. Zawojska, a Dudzinski, R. Kinasz, and D. Wygledowska-Promienska, "Measurement of pupil reactivity using fast pupillometry", Physiological measurement, vol. 28, no. 1, pp. 61–72, Jan. 2007.
[9] S. Heindl, J. Struck, P. Wellhöner, F. Sayk, and C. Dodt, "Effect of facial cooling and cold air inhalation on sympathetic nerve activity in men", Respiratory physiology & neurobiology, vol. 142, no. 1, pp. 69–80, Aug. 2004.
[10] R. G. Victor, W. N. Leimbach, D. R. Seals, B. G. Wallin, and a. L. Mark, "Effects of the cold pressor test on muscle sympathetic nerve activity in humans", Hypertension, vol. 9, no. 5, pp. 429–436, May 1987.
[11] D. F. Fotiou, V. Stergiou, D. Tsiptsios, C. Lithari, M. Nakou, and a Karlovasitou, "Cholinergic deficiency in Alzheimer's and Parkinson's disease: evaluation with pupillometry", International journal of psychophysiology : official journal of the International Organization of Psychophysiology, vol. 73, no. 2, pp. 143–9, Aug. 2009.
[12] V. Stergiou, D. Fotiou, D. Tsiptsios, B. Haidich, M. Nakou, C. Giantselidis, and A. Karlovasitou, "Pupillometric findings in patients with Parkinson's disease and cognitive disorder", International journal of psychophysiology : official journal of the International Organization of Psychophysiology, vol. 72, no. 2, pp. 97–101, May 2009.
[13] G. Leal, "Desenvolvimento de um Pupilómetro", Master Degree Thesis, Faculdade de Ciências e Tecnologia da Universidade Nova de Lisboa, 2008.
[14] C. M. Rocco S, "Singular spectrum analysis and forecasting of failure time series", Reliability Engineering & System Safety, vol. 114, pp. 126–136, Jun. 2013.
[15] N. Golyandina, V. Nekrutkin, and A. A. Zhigljavsky, "Basic SSA", inAnalysis of Time Series Structure - SSA and Related Techniques, New York: Chapman & Hall/CRC, 2001.
[16] G. Leal, C. Neves and P. Vieira, "Pupillometry: Development of Equipment for Studies of Autonomic Nervous System." IFIP 372, pp.553-562, 2012.
[17] N. Golyandina, V. Nekrutkin, and K. Braulov, "Caterpillar-SSA: Time series analysis and forecasting." [Online]. Available: http://www.gistatgroup.com/cat/programs.html.
[18] H. Hassani, "Singular Spectrum Analysis: Methodology and Comparison", Journal of Data Science, vol. 5, no. 4991, pp. 239–257, 2007.
[19] L. Sherwood, Fundamentals of Physiology: A Human Perspective, 3rd ed. Thomson Brooks/Cole, 2006, p. 380.
[20] V. Fuster, R. A. O'Rouke, and R. W. Alexander, Hurst's the Heart, 10th ed. McGraw-Hill, 2001, pp. 78–79.